Nano Nexus & Applications

www.nna.reapress.com

Research Expansion Alliance

Nano. Nex. App. Vol. 1, No. 2 (2026) 127–143.

Paper Type: Original Article

Numerical Investigation of Heat Transfer Enhancement in a Backward-Facing Step Channel Using Jet Injection and Al_2O_3/CMC Nanofluids

Ali Bozorgimanesh*

Department of Mechanical Engineering, Daneshpajoohan Pishroo Higher Education Institute, Isfahan, Iran; ali.bozorgimanesh@gmail.com.

Citation:

Received: 08 November 2025 *Revised: 11 February 2026* *Accepted: 16 April 2026*	Bozorgimanesh, A. (2026). Numerical investigation of heat transfer enhancement in a backward-facing step channel using jet injection and Al_2O_3/CMC nanofluids. *Nano Nexus & Applications, 1*(2), 127-143.

Abstract

This study numerically investigates heat transfer enhancement in a Backward-Facing Step (BFS) channel subjected to jet injection using a non-Newtonian Aluminum Oxide/Carboxymethyl Cellulose (Al_2O_3/CMC) nanofluid. The flow is assumed to be steady, laminar, incompressible, and two-dimensional. The rheological behavior of the CMC solution is modeled using the power-law model, while the governing equations of mass, momentum, and energy are solved using the Finite Volume Method (FVM). The effects of Reynolds number, jet injection angle, jet momentum ratio, nanoparticle volume fraction, and fluid rheology on flow structure and thermal performance are systematically analyzed. The numerical model is first validated against previously published experimental and numerical data, showing good agreement. The results indicate that increasing the Reynolds number significantly enhances convective heat transfer due to stronger recirculation and thinner thermal boundary layers. The use of a non-Newtonian CMC solution improves thermal performance compared with Newtonian water, while the addition of Al_2O_3 nanoparticles further increases the heat transfer rate because of enhanced effective thermal conductivity. The jet injection parameters strongly affect the flow field and thermal characteristics. Appropriate jet injection angles and momentum ratios intensify fluid mixing near the heated wall and lead to substantial heat transfer enhancement. The thermal-hydraulic Performance Evaluation Criterion (PEC) demonstrates that the combined use of jet injection and Al_2O_3/CMC nanofluids can provide superior overall performance compared with conventional cooling configurations. The findings confirm the potential of jet-assisted non-Newtonian nanofluids for improving thermal management in BFS channels and similar engineering systems.

Keywords: Carboxymethyl cellulose, Nanofluid, Jet injection, Reynolds number, Heat transfer enhancement, Nusselt number.

1 | Introduction

Heat transfer enhancement has become one of the most important challenges in modern thermal engineering due to the increasing demand for compact and high-performance thermal systems[1–3]. Applications such as electronic cooling devices, compact heat exchangers, energy conversion systems, chemical reactors, and

Corresponding Author: ali.bozorgimanesh@gmail.com

https://doi.org/10.48314/nna.vi.65

aerospace thermal management require efficient techniques to improve heat transfer while maintaining acceptable pressure losses [4]. Consequently, considerable research efforts have been devoted to developing both passive and active enhancement techniques for improving thermal performance in internal flow systems. Among the various geometrical configurations used to investigate convective heat transfer phenomena, the Backward-Facing Step (BFS) channel has attracted significant attention because of its complex flow structure and practical engineering relevance [5], [6]. Flow over a BFS is characterized by boundary layer separation, formation of a recirculation zone, and subsequent flow reattachment. These flow phenomena strongly influence local wall shear stress, pressure distribution, and heat transfer characteristics [1]. Due to its relatively simple geometry and complex fluid-dynamic behavior, the BFS configuration has become a benchmark problem for validating numerical methods and studying separated flows [7–9]. Several studies have demonstrated that the thermal performance of BFS channels can be significantly affected by flow control techniques. In particular, the manipulation of recirculation zones and reattachment length has been shown to provide an effective means of improving heat transfer rates [10]. Both passive methods, such as ribs, vortex generators, and surface modifications, and active methods, including synthetic jets, suction, and jet injection, have been investigated extensively. Among these approaches, jet injection has emerged as an attractive active flow-control strategy because it can directly modify the separated flow region, enhance momentum exchange, and promote fluid mixing. The injected jet interacts with the primary flow, alters the vortex structure downstream of the step, and can substantially improve thermal performance [2], [11–14]. In parallel with advances in flow-control techniques, the development of advanced heat transfer fluids has opened new opportunities for enhancing thermal transport processes. Conventional heat transfer fluids such as water, ethylene glycol, and oils generally possess low thermal conductivity compared with metallic and ceramic materials. This limitation restricts the thermal efficiency of many engineering systems. To overcome this challenge, nanofluids have been proposed as a new class of working fluids formed by dispersing nanoparticles in a base fluid. Numerous experimental and numerical investigations have reported that the addition of nanoparticles can improve thermal conductivity, increase convective heat transfer coefficients, and enhance the overall thermal performance of heat transfer equipment [2], [12–16].

Among various nanoparticle materials, Aluminum Oxide (Al_2O_3) nanoparticles have been widely employed due to their favorable thermal properties, chemical stability, and relatively low cost. Al_2O_3/water nanofluids have demonstrated considerable potential for improving heat transfer performance in channels, heat exchangers, and cooling systems. The enhancement mechanisms associated with nanofluids are generally attributed to increased effective thermal conductivity, Brownian motion of nanoparticles, micro-scale mixing effects, and modifications in the thermal boundary layer structure [5]. While most previous studies have focused on Newtonian base fluids, many industrial fluids exhibit non-Newtonian behavior. Polymer solutions, biological fluids, food products, slurries, paints, and numerous process fluids cannot be accurately described using Newtonian constitutive relations [7–9]. The rheological characteristics of non-Newtonian fluids significantly influence velocity distribution, wall shear stress, flow separation, and heat transfer behavior. In particular, shear-thinning fluids, commonly represented by the power-law model, exhibit a decrease in apparent viscosity with increasing shear rate. This behavior can substantially alter the hydrodynamic and thermal characteristics of separated flows. The combined application of nanofluids and non-Newtonian fluids has recently attracted growing attention because it offers the possibility of simultaneously benefiting from enhanced thermal conductivity and favorable rheological properties [13–17]. Several researchers have investigated the behavior of non-Newtonian nanofluids in different thermal systems and reported considerable improvements in heat transfer performance. Nevertheless, the interaction between non-Newtonian rheology, nanoparticle transport, and separated flow structures remains insufficiently understood, particularly in complex geometries such as BFS channels [15].

Previous investigations on BFS flows have mainly concentrated on Newtonian fluids without active flow control, while studies involving nanofluids have generally focused on the effects of nanoparticle concentration and Reynolds number. Similarly, research concerning non-Newtonian fluids in BFS geometries remains relatively limited. Furthermore, although jet injection has been recognized as an effective flow-control technique, the combined influence of jet injection and non-Newtonian nanofluids on flow separation and heat transfer enhancement has received comparatively little attention in the literature [18]. The coupling between jet-induced flow modification, nanoparticle-enhanced thermal transport, and non-Newtonian rheology may lead to complex interactions that cannot be predicted solely from existing studies. Therefore, the present study aims to numerically investigate the combined effects of jet injection and non-Newtonian Al_2O_3/CMC nanofluid flow in a BFS channel under laminar conditions. A two-dimensional numerical model based on the Finite Volume Method (FVM) is employed to solve the governing continuity, momentum, and energy equations. The rheological behavior of the working fluid is described using the power-law model, while the thermophysical properties of the nanofluid are evaluated for different nanoparticle volume fractions [15–20]. The effects of Reynolds number, nanoparticle concentration, jet injection conditions, and flow behavior characteristics on the flow field and thermal performance are systematically analyzed. Particular attention is devoted to the evolution of the recirculation zone, heat transfer enhancement, pressure drop characteristics, and overall thermal-hydraulic performance [21].

The findings of this work provide further insight into the coupled mechanisms of active flow control and advanced heat transfer fluids in separated flow systems. The results may contribute to the design and optimization of compact thermal devices, electronic cooling systems, and heat exchangers where enhanced thermal performance and efficient flow management are simultaneously required.

2|Materials and Methods

2.1|Physical Model

A two-dimensional BFS channel was considered to investigate the combined effects of jet injection and non-Newtonian nanofluid flow on heat transfer enhancement and flow control. The computational domain consisted of an upstream section, a sudden expansion region created by the BFS, and a downstream section where flow reattachment occurred. To ensure fully developed conditions before the step and eliminate outlet boundary effects, the lengths of the upstream and downstream sections were selected as 20H and 50H, respectively, where H denotes the step height. A jet nozzle was positioned at the step edge and injected fluid into the main flow at a prescribed angle (θ) relative to the horizontal direction. The lower wall downstream of the step was subjected to a uniform heat flux, while the upper wall was assumed adiabatic. All solid boundaries satisfied the no-slip condition. Owing to the relatively low Reynolds number range considered in this study ($Re \leq 500$), the flow was assumed to be two-dimensional and laminar.

2.2|Working Fluid and Thermophysical Properties

The working fluid consisted of a non-Newtonian aqueous solution of Carboxymethyl Cellulose (CMC) containing Al_2O_3 nanoparticles. The suspension was modeled as a homogeneous single-phase nanofluid under thermal equilibrium conditions. Al_2O_3 nanoparticles were selected because of their high thermal conductivity, chemical stability, and widespread application in thermal engineering systems.

The effective density of the nanofluid was calculated as (*Eq. (1)*) [9]:

$$\rho_{nf} = (1-\varphi)\rho_f + \varphi\rho_p, \tag{1}$$

where φ represents the nanoparticle volume fraction, while subscripts nf, f, and p refer to nanofluid, base fluid, and nanoparticle, respectively.

The effective heat capacity was determined using (*Eq. (2)*) [11]:

$$(\rho c_P)_{nf} = (1-\varphi)(\rho c_P)_f + \varphi(\rho c_P)_p. \tag{2}$$

The effective thermal conductivity was calculated using an appropriate nanofluid thermal conductivity model based on the nanoparticle concentration. The thermophysical properties of water, Al_2O_3 nanoparticles, and nanofluids at different volume fractions were adopted from available experimental correlations and previous studies.

2.3 | Rheological Model

The CMC solution exhibits shear-thinning behavior and therefore cannot be accurately represented by Newtonian constitutive equations. The rheological behavior of the fluid was modeled using the Power-Law model (*Eq. (3)*) [9]:

$$\tau = K\dot{\gamma}^{(n-1)}, \tag{3}$$

where τ is the shear stress, $\dot{\gamma}$ is the shear rate, K is the consistency index, and n is the flow behavior index. The apparent viscosity was calculated as (*Eq. (4)*) [9]:

$$\mu app = K\dot{\gamma}\hat{}(n-1). \tag{4}$$

For values of n less than unity, the fluid exhibits pseudoplastic (shear-thinning) behavior. This rheological model has been widely used to describe CMC solutions and other polymeric fluids encountered in thermal applications.

2.4 | Governing Equations

The numerical simulations were performed assuming steady-state, incompressible, laminar, and two-dimensional flow conditions. Furthermore, thermal equilibrium between the nanoparticles and the base fluid was assumed. The governing equations include conservation of mass, momentum, and energy.

2.4.1 | Continuity Equation

The conservation of mass is expressed as (*Eq. (5)*) [10]:

$$\nabla . V = 0, \tag{5}$$

where V is the velocity vector.

2.4.2 | Momentum Equations

The momentum equations in Cartesian coordinates are given by (*Eq. (6)*) [11]:

$$\rho nf(V.\nabla)V = -\nabla P + \nabla(\mu app \nabla V), \tag{6}$$

where P denotes pressure and μapp represents the apparent viscosity obtained from the power-law model.

2.4.3 | Energy Equation

The energy equation can be expressed as (*Eq. (7)*) [2]:

$$\rho nfCp, nf(V \cdot \nabla T) = \nabla \cdot (knf \nabla T), \tag{7}$$

where T is the temperature and knf is the effective thermal conductivity of the nanofluid.

2.5 | Boundary Conditions

A uniform velocity profile and constant temperature were imposed at the channel inlet. At the outlet boundary, fully developed flow conditions were assumed, and all axial gradients were set equal to zero. The lower wall downstream of the step was subjected to a constant heat flux condition (*Eq. (8)*) [10]:

$$-\mathrm{knf}\left(\frac{\partial \mathrm{T}}{\partial \mathrm{y}}\right) = \mathrm{q}''. \quad (8)$$

The upper wall was considered adiabatic (*Eq. (9)*) [9]:

$$\partial \mathrm{T}/\partial \mathrm{n} = 0. \quad (9)$$

The no-slip boundary condition was applied to all solid walls, resulting in zero velocity components at the wall surfaces (u=v=0). The injected jet was introduced into the channel with a prescribed velocity and injection angle. Various jet momentum ratios and injection angles were considered to evaluate their effects on the flow structure and thermal performance.

2.6 | Numerical Procedure

The governing equations were discretized using the FVM. The computational domain was divided into structured quadrilateral control volumes to accurately capture the complex flow features, including flow separation and reattachment phenomena occurring near the BFS. The pressure-velocity coupling was achieved using the SIMPLE algorithm. The convective terms were discretized using a second-order upwind scheme to provide an accurate prediction of the transported quantities, while the diffusive terms were evaluated using the second-order central differencing scheme. The resulting algebraic equations were solved iteratively until a converged solution was obtained. The convergence criteria were defined based on the normalized residuals, with values of 10^{-6} for the continuity and momentum equations and 10^{-8} for the energy equation. All numerical simulations were performed under steady-state conditions.

2.7 | Grid Independence Study

To ensure numerical accuracy and eliminate the influence of mesh size on the predicted results, a grid independence analysis was conducted using several structured meshes with increasing cell numbers. The average Nusselt number and reattachment length were selected as the primary monitoring parameters. When the variation between two consecutive mesh refinements became less than 1%, the numerical solution was considered independent of grid size. The optimum mesh was then adopted for all subsequent simulations to achieve a balance between computational cost and numerical accuracy.

2.8 | Model Validation

The numerical model was validated against previously published experimental and numerical results for BFS flows available in the literature. Comparisons were performed for velocity profiles, reattachment length, and Nusselt number distributions. Good agreement was obtained between the present predictions and reference data, confirming the accuracy and reliability of the numerical methodology. The maximum deviation between the present results and benchmark data remained within acceptable engineering limits, demonstrating the capability of the developed model to accurately predict flow separation and heat transfer characteristics in BFS channels.

2.9 | Performance Evaluation Criterion

To assess the combined effects of heat transfer enhancement and pressure loss, a thermal-hydraulic Performance Evaluation Criterion (PEC) was employed. The PEC parameter was defined as (*Eq. (10)*) [11]:

$$\mathrm{PEC} = \frac{\mathrm{Nu}/\mathrm{Nu_0}}{\left(\frac{\mathrm{f}}{\mathrm{f_0}}\right)^{1/3}}, \tag{10}$$

where Nu and f denote the average Nusselt number and friction factor for the enhanced configuration, while Nu0 and f0 correspond to the reference case. A PEC value greater than unity indicates that the heat transfer enhancement outweighs the associated pressure-drop penalty and therefore represents an overall performance improvement.

3 | Results and Discussion

3.1 | Validation of the Numerical Model

Prior to the parametric investigation, the numerical model was validated against previously published benchmark studies in order to assess its capability in predicting both heat transfer and flow characteristics. Two independent validation cases were considered. First, the thermal model was validated by comparing the predicted local and average Nusselt numbers with the numerical results reported by Santra et al. [14] for laminar non-Newtonian nanofluid flow in a heated microchannel. In the reference study, the Nusselt number distribution along the heated wall and the average Nusselt number were reported for Reynolds numbers ranging from 10 to 200. The same operating conditions were reproduced in the present simulation, and the obtained results were compared with the published data. *Fig. 1.a* presents the comparison between the present numerical predictions and the results of Santra et al. [14]for both the local and average Nusselt numbers. As observed, the local Nusselt number decreases gradually along the heated wall due to the growth of the thermal boundary layer, while the average Nusselt number increases with increasing Reynolds number. The numerical predictions closely follow the reference data throughout the investigated Reynolds number range. The excellent agreement confirms that the adopted governing equations, thermophysical property models, and numerical discretization schemes accurately capture the thermal transport behavior of non-Newtonian nanofluids. A second validation was performed to evaluate the capability of the model in predicting separated flow characteristics in a BFS geometry. For this purpose, the velocity profiles downstream of the step were compared with the experimental measurements reported by Armaly et al. [15] at Reynolds number Re=389. The benchmark geometry consisted of a BFS with an expansion ratio of approximately 1.94, and velocity distributions were reported at several downstream locations. The same configuration was simulated in the present study, and the predicted velocity profiles were extracted at corresponding streamwise sections. The comparison shown in *Fig. 1.b* demonstrates that the present numerical results accurately reproduce the experimental velocity distributions. In particular, the model successfully predicts the reverse-flow region immediately downstream of the step as well as the subsequent recovery of the velocity profile toward the fully developed state. The agreement between numerical and experimental data indicates that the present computational approach is capable of capturing the essential flow features associated with separation, recirculation, and reattachment phenomena in BFS flows.

The close correspondence between the present predictions and the benchmark thermal and hydrodynamic data confirms the reliability of the numerical methodology. Therefore, the developed model can be confidently employed for the subsequent investigation of the effects of non-Newtonian behavior, jet injection parameters, Reynolds number, and nanoparticle concentration on flow control and heat transfer enhancement in the BFS channel.

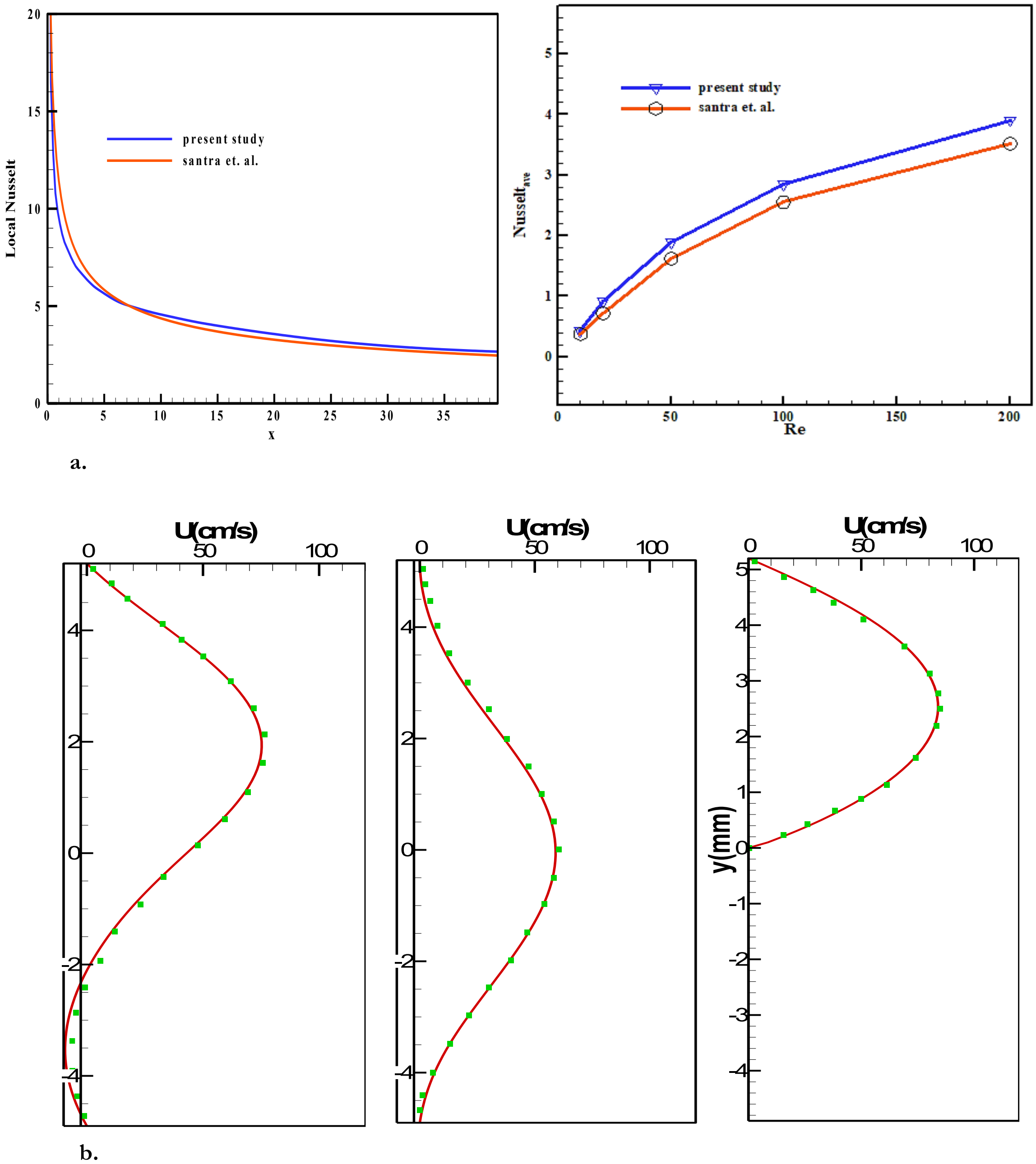

Fig. 1. Validation of the numerical model; a. Nusselt number comparison with Santra et al. [14], and b. velocity profiles comparison with Armaly et al. [15].

3.2 | Effect of Reynolds Number

The Reynolds number is one of the most influential parameters governing the hydrodynamic and thermal characteristics of flow in a BFS channel. Variations in Reynolds number directly affect the momentum transport mechanism, recirculation zone development, boundary layer growth, and heat transfer performance. Therefore, the effect of Reynolds number on the flow structure and thermal behavior of the non-Newtonian nanofluid was systematically investigated. *Fig. 2* illustrates the streamline contours obtained at different Reynolds numbers. As the Reynolds number increases, the inertia forces become increasingly dominant over viscous effects, resulting in significant modifications of the separated flow region downstream of the step. The size and intensity of the primary recirculation zone increase with Reynolds number, while the reattachment point moves further downstream. This behavior can be attributed to the stronger momentum of the incoming flow, which enhances flow separation immediately after the sudden expansion.

The increase in Reynolds number also alters the velocity gradients near the heated wall. Stronger shear layers are generated at higher Reynolds numbers, promoting fluid mixing between the recirculation region and the core flow. Consequently, the thermal boundary layer becomes thinner, and heat transfer is intensified. The influence of Reynolds number on the average Nusselt number is presented in *Fig. 3*. It can be observed that the average Nusselt number increases monotonically with increasing Reynolds number. At higher Reynolds numbers, the enhanced fluid motion increases convective transport and improves thermal energy exchange between the heated wall and the working fluid. Furthermore, stronger recirculation enhances the renewal of fluid particles near the wall, which contributes to higher local temperature gradients and consequently larger Nusselt numbers. The observed enhancement in heat transfer is consistent with the classical behavior of forced convection flows, where increasing Reynolds number leads to improved thermal performance. However, the increase in Reynolds number is generally accompanied by a higher pressure drop due to larger wall shear stresses. Therefore, a comprehensive thermal-hydraulic assessment is required to determine the optimal operating conditions.

The results indicate that Reynolds number plays a dominant role in controlling both the flow structure and thermal performance of the BFS channel. Higher Reynolds numbers promote stronger recirculation, thinner thermal boundary layers, and enhanced convective heat transfer, leading to a substantial increase in the average Nusselt number.

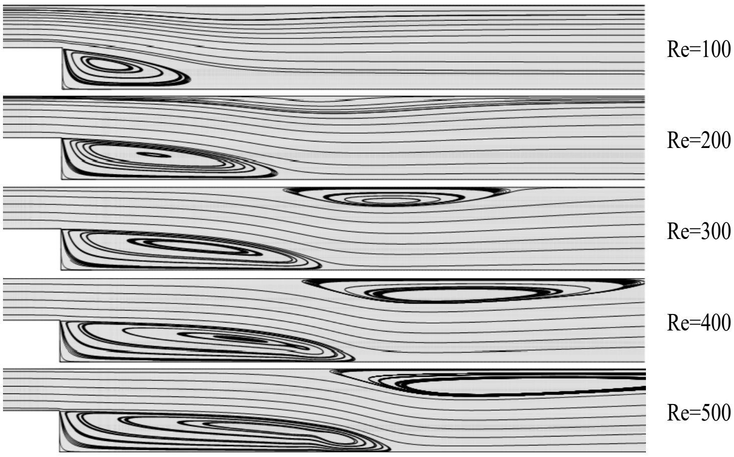

Fig. 2. Streamline patterns for different Reynolds numbers in the BFS channel.

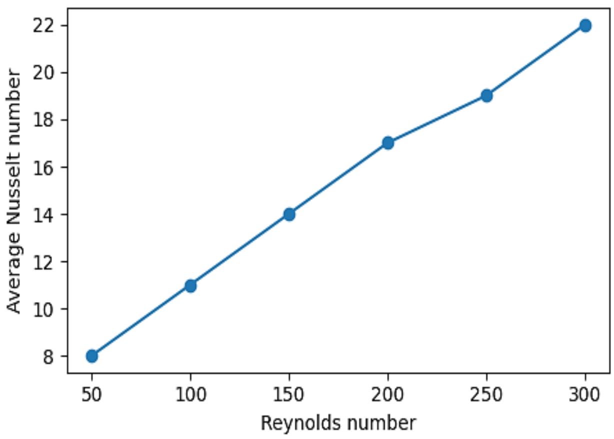

Fig. 3. Variation of the average Nusselt number with Reynolds number.

3.3|Effect of Nanoparticle Volume Fraction

The influence of nanoparticle volume fraction on the thermal and hydrodynamic performance of the BFS channel was investigated by varying the concentration of Al_2O_3 nanoparticles while maintaining the remaining operating conditions constant. The addition of nanoparticles modifies the effective thermophysical properties of the working fluid, particularly the thermal conductivity, which directly affects heat transfer characteristics. *Fig. 4* presents the streamline patterns for different nanoparticle volume fractions. As the nanoparticle concentration increases from φ=0.5% to φ=1.5%, only minor changes can be observed in the overall flow structure and recirculation region. The streamline distributions indicate that the addition of nanoparticles has a negligible influence on the hydrodynamic behavior of the flow. Therefore, the thermal enhancement associated with increasing nanoparticle concentration is primarily attributed to improvements in the thermophysical properties of the nanofluid rather than significant modifications of the flow field. The variation of the average Nusselt number with nanoparticle volume fraction is illustrated in *Fig. 5*. The results indicate that increasing the nanoparticle concentration leads to a continuous enhancement in convective heat transfer performance. The presence of Al_2O_3 nanoparticles increases the effective thermal conductivity of the suspension, thereby strengthening the heat transport mechanism within the channel. As a result, larger wall temperature gradients are maintained, leading to higher Nusselt numbers. The enhancement becomes more pronounced at higher Reynolds numbers, where stronger fluid mixing further amplifies the beneficial effect of the nanoparticles. Although the addition of nanoparticles improves heat transfer performance, it also affects the flow resistance by altering the effective viscosity and density of the working fluid. Therefore, the overall performance cannot be assessed solely on the basis of heat transfer enhancement. To address this issue, the thermal-hydraulic Performance Criterion (PEC) was evaluated and is presented in *Fig. 5*.

As shown in *Fig. 5*, the PEC values remain greater than unity throughout the investigated range of nanoparticle concentrations, indicating that the improvement in heat transfer outweighs the corresponding increase in pressure drop. However, the rate of improvement gradually decreases at higher volume fractions, suggesting that excessive nanoparticle loading may not provide proportional thermal benefits. This observation highlights the existence of an optimum nanoparticle concentration that balances heat transfer enhancement and hydraulic losses. The results demonstrate that increasing the nanoparticle volume fraction effectively enhances thermal performance in the BFS channel. The improved thermal conductivity of the nanofluid leads to higher Nusselt numbers and favorable thermal-hydraulic performance, confirming the potential of Al_2O_3/CMC nanofluids for advanced cooling applications.

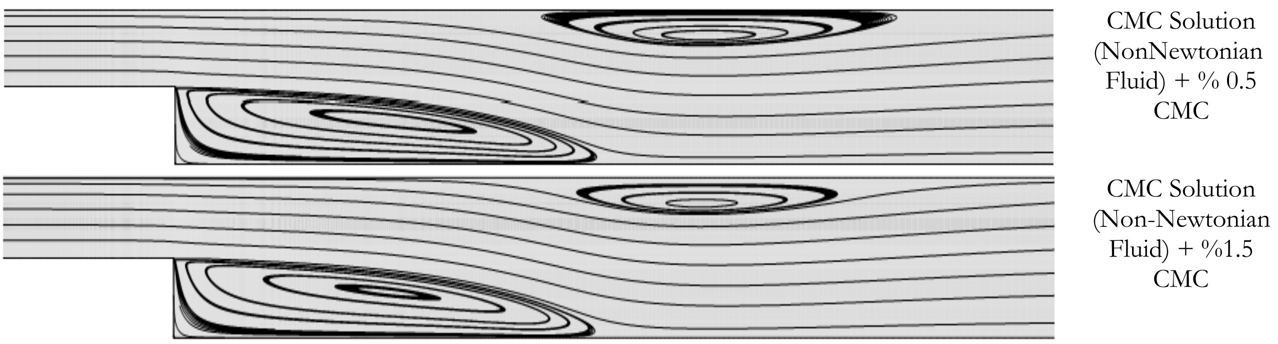

Fig. 4. Streamline patterns for different nanoparticle volume fractions (φ = 0.5% and 1.5%) at Re = 300, j = 4, and θ = 0.

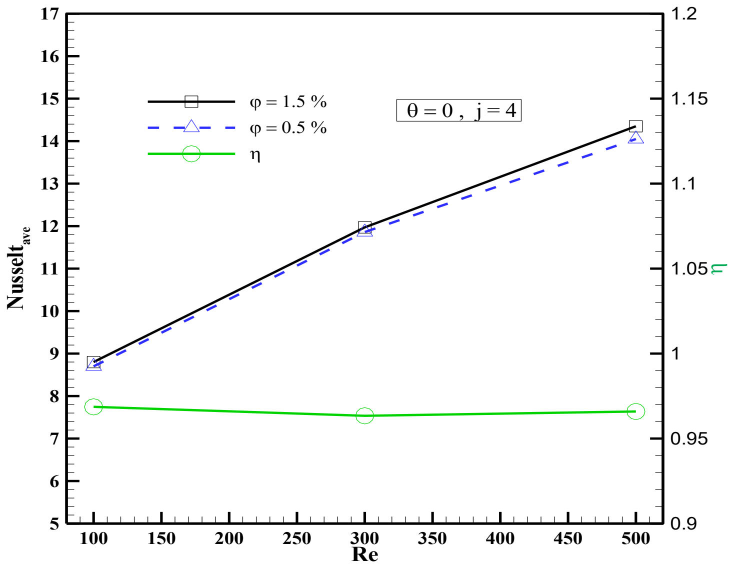

Fig. 5. Variation of average Nusselt number and PEC for different nanoparticle volume fractions.

3.4 | Effect of Non-Newtonian Behavior

The influence of fluid rheology on the flow and heat transfer characteristics of the BFS channel was investigated by comparing Newtonian water and a non-Newtonian CMC solution under identical operating conditions. This comparison was performed to isolate the effect of shear-thinning behavior on the thermal and hydrodynamic performance of the system. *Fig. 6* presents the streamline patterns obtained for Newtonian water and the non-Newtonian CMC solution. It can be observed that the general structure of the recirculation region remains similar for both fluids. However, the size and intensity of the recirculation zone are slightly affected by the rheological properties of the fluid. The non-Newtonian CMC solution exhibits shear-thinning behavior, which reduces the apparent viscosity in regions of high shear rate. As a result, momentum transport is enhanced near the separation and reattachment zones, leading to a more favorable flow structure compared with the Newtonian water case. The effect of fluid rheology on heat transfer performance is illustrated in *Fig. 7*. The results indicate that the average Nusselt number increases when water is replaced by the CMC solution. This enhancement can be attributed to the shear-thinning behavior of the CMC solution, which reduces viscous resistance in high-shear regions and promotes stronger mixing near the heated wall. Consequently, thermal energy is transported more effectively from the heated surface to the bulk fluid, resulting in improved convective heat transfer performance. The results clearly demonstrate that fluid rheology plays a significant role in determining both flow behavior and heat transfer characteristics in BFS channels. Compared with Newtonian water, the non-Newtonian CMC solution provides enhanced heat transfer performance while maintaining a similar flow structure. These findings highlight the potential of shear-thinning fluids for improving thermal management in engineering systems involving separated flows.

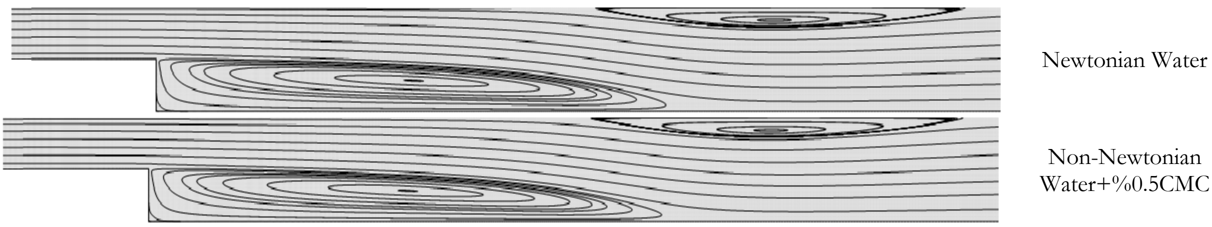

Fig. 6. Streamline patterns for Newtonian water and non-Newtonian CMC solution at Re = 300.

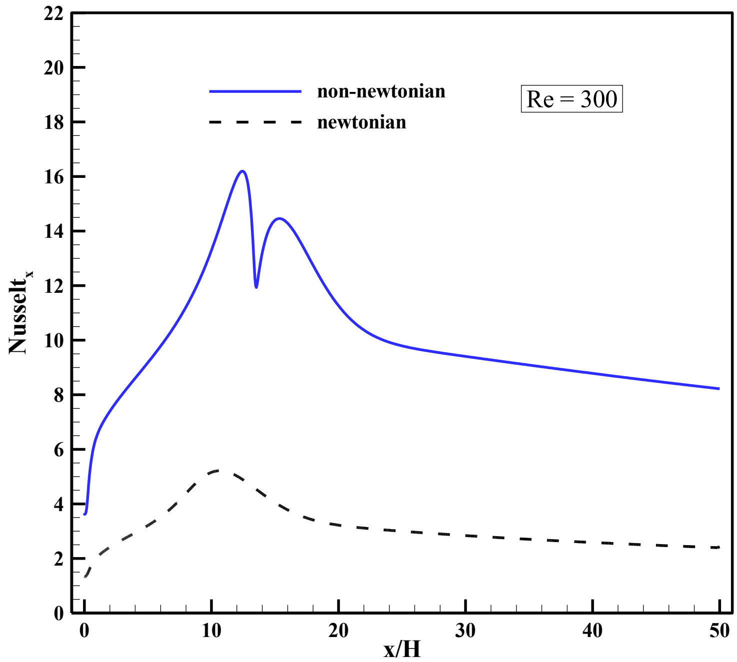

Fig. 7. Local Nusselt number distribution along the heated wall for Newtonian water and non-Newtonian CMC solution at Re = 300.

3.5 | Effect of Jet Injection Angle

The injection angle of the jet is an important geometric parameter affecting the interaction between the injected flow and the main stream within the BFS channel. Variations in jet injection angle alter the momentum distribution, recirculation structure, and thermal mixing process, thereby influencing the overall thermal-hydraulic performance. *Fig. 8* presents the streamline patterns for different jet injection angles. It can be observed that changing the jet angle significantly modifies the flow field downstream of the step. At smaller injection angles, the jet tends to remain attached to the heated wall, promoting stronger interaction with the recirculation region. As the injection angle increases, the jet penetrates deeper into the core flow and weakens the near-wall mixing mechanism. Consequently, noticeable changes occur in the size and intensity of the recirculation zone. The influence of jet angle on heat transfer characteristics is illustrated in *Fig. 9*. The local Nusselt number distributions reveal that the injection angle strongly affects wall heat transfer. Moderate injection angles generate stronger mixing between the cold jet and the heated fluid near the wall, resulting in higher temperature gradients and improved convective heat transfer. However, excessively large injection angles reduce the direct interaction between the jet and the heated surface, leading to a reduction in thermal enhancement. To evaluate the overall system performance, the variation of average Nusselt number and PEC with jet angle is presented in *Fig. 10*. The results indicate that both heat transfer enhancement and thermal-hydraulic performance depend strongly on the injection angle. An optimum injection angle is observed, at which the beneficial effects of flow mixing outweigh the associated pressure-drop penalty. Beyond this optimum value, the increase in hydraulic losses becomes more significant, and the PEC gradually decreases.

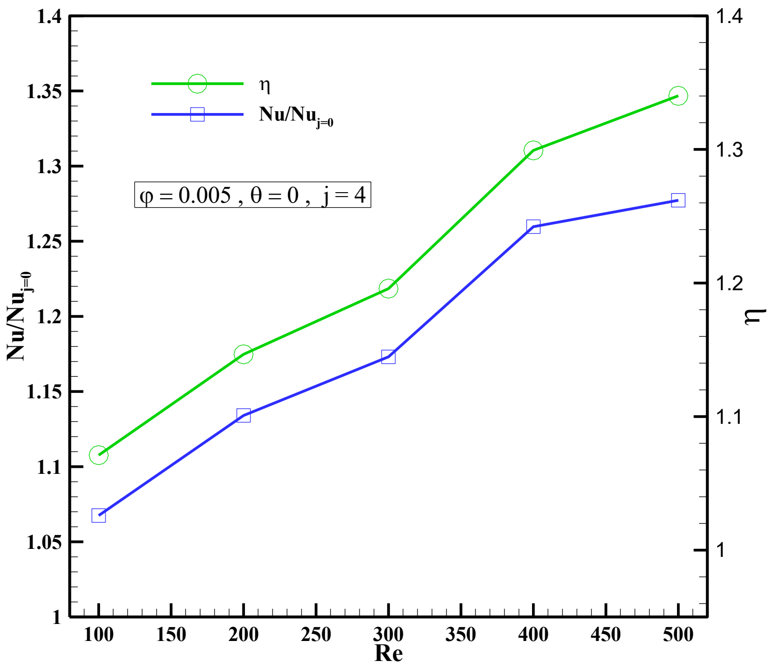

Fig. 8. Streamline patterns for different jet injection angles.

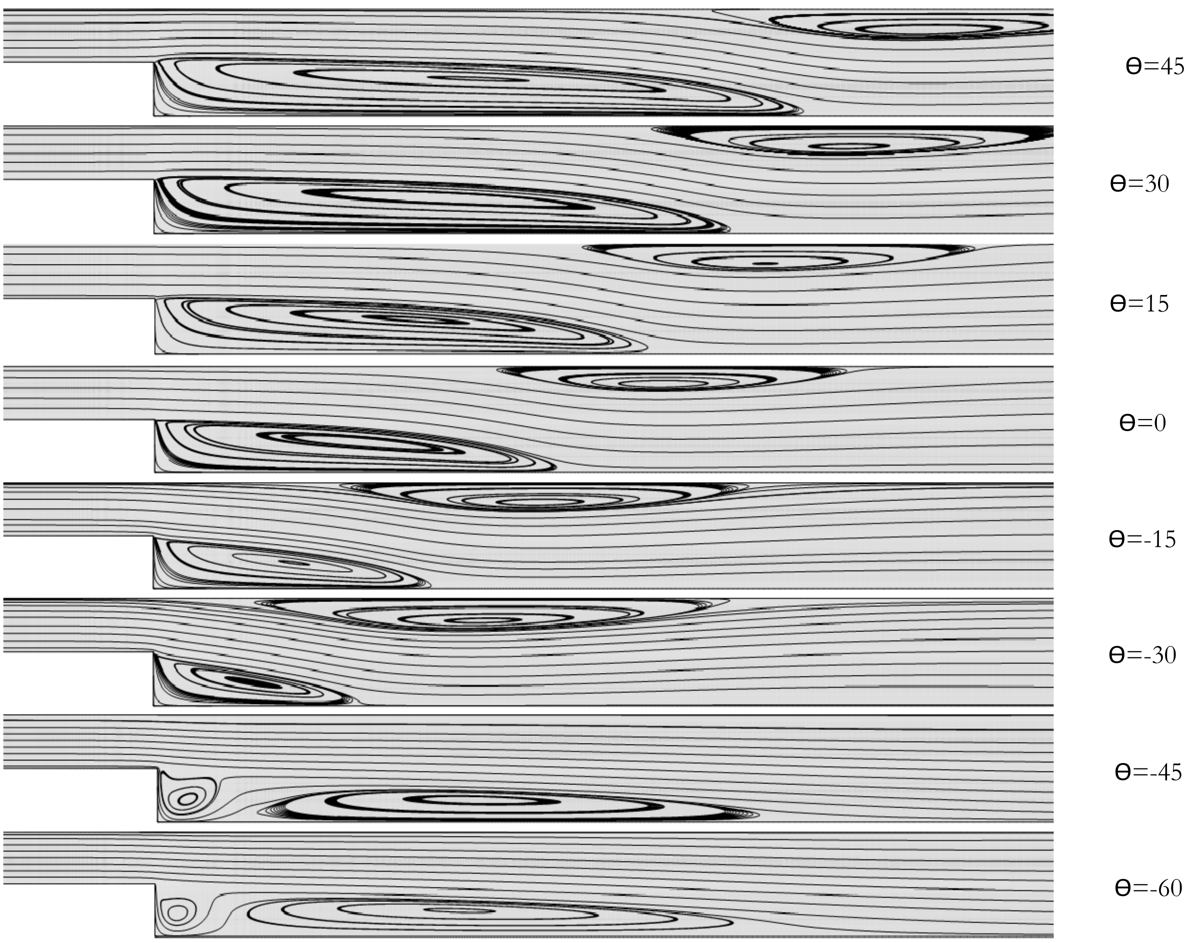

Fig. 9. Local Nusselt number distributions along the heated wall for different jet injection angles.

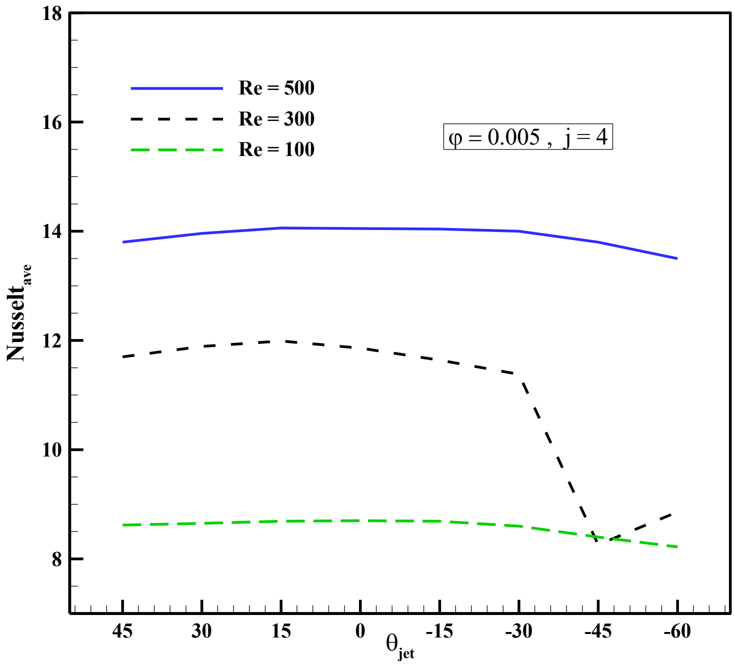

Fig. 10. Variation of average Nusselt number and PEC with jet injection angle.

3.6 | Effect of Jet Momentum Ratio

The jet momentum ratio is one of the most influential parameters governing the interaction between the injected jet and the main channel flow. Variations in the momentum ratio modify the jet penetration intensity, flow mixing process, and thermal performance of the BFS channel. *Fig. 11* presents the variation of the average Nusselt number for different jet momentum ratios at various Reynolds numbers. The results indicate that increasing the jet momentum ratio enhances the heat transfer performance due to stronger interaction between the injected jet and the main flow. A higher momentum ratio provides greater jet kinetic energy, which improves fluid mixing near the heated wall and disrupts the thermal boundary layer. Consequently, the convective heat transfer rate increases, resulting in higher average Nusselt numbers. The enhancement becomes more significant at higher Reynolds numbers, where stronger inertial effects promote deeper jet penetration and more intensive mixing within the recirculation region. However, increasing the jet momentum ratio also increases flow disturbances and may lead to higher pressure losses. *Fig. 12* illustrates the variation of the thermal-hydraulic PEC for different jet momentum ratios. The PEC results demonstrate that increasing the momentum ratio does not always lead to proportional improvement in overall performance. Although stronger jet injection enhances heat transfer, excessive momentum ratios increase hydraulic penalties due to higher flow resistance. Therefore, an optimum jet momentum ratio exists, providing the best balance between heat transfer enhancement and pressure-drop increase. The results confirm that the jet momentum ratio plays a crucial role in controlling the thermal performance of BFS channels. Proper adjustment of this parameter can significantly enhance heat transfer while maintaining acceptable hydraulic efficiency.

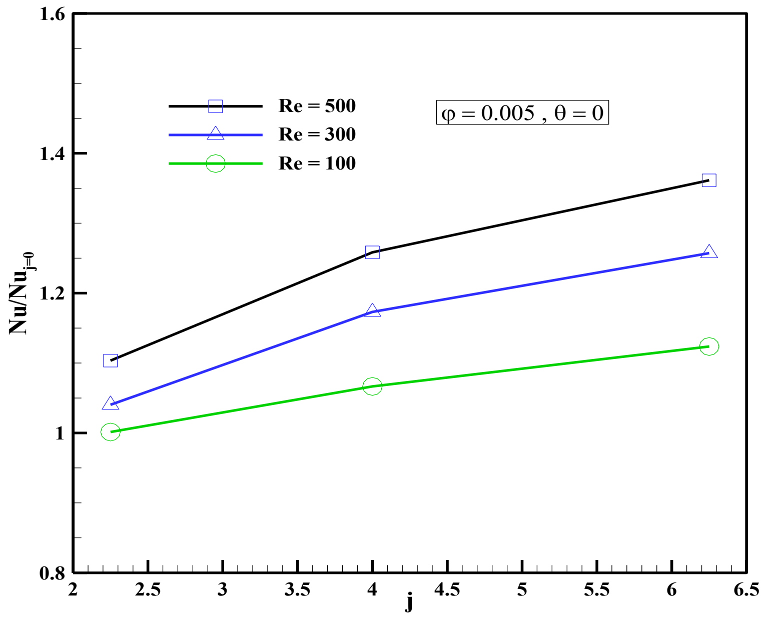

Fig. 11. Variation of average Nusselt number for different jet momentum ratios at various Reynolds numbers.

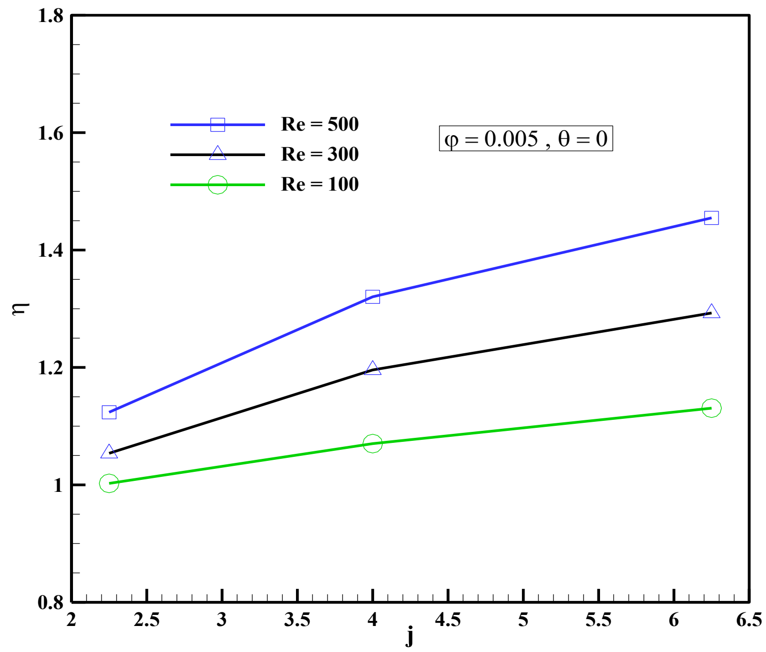

Fig. 12. Variation of PEC for different jet momentum ratios at various Reynolds numbers.

4 | Conclusion

This study numerically investigated the thermal and hydrodynamic performance of a BFS channel subjected to jet injection using a non-Newtonian Al_2O_3/CMC nanofluid. The effects of Reynolds number, nanoparticle volume fraction, fluid rheology, jet injection angle, and jet momentum ratio on flow structure and heat transfer characteristics were systematically analyzed using the FVM. The numerical model was first validated against available benchmark data and demonstrated good agreement with previously published experimental and numerical results, confirming the reliability of the adopted methodology. The results revealed that increasing

the Reynolds number significantly enhanced heat transfer performance by intensifying fluid mixing, reducing thermal boundary layer thickness, and increasing both local and average Nusselt numbers. The use of the non-Newtonian CMC solution provided superior thermal behavior compared with Newtonian water due to its shear-thinning characteristics, which improved momentum and heat transport in regions with high velocity gradients. Furthermore, the incorporation of Al_2O_3 nanoparticles increased the effective thermal conductivity of the working fluid and consequently improved the heat transfer rate throughout the channel.
The study also demonstrated that jet injection is an effective technique for thermal enhancement in BFS configurations. Variations in jet injection angle considerably affected the flow structure and recirculation region, leading to significant changes in thermal performance. A suitable injection angle was found to provide a favorable balance between enhanced heat transfer and hydraulic losses. Similarly, increasing the jet momentum ratio strengthened jet penetration and intensified mixing between the injected flow and the main stream, resulting in improved cooling performance. However, excessive momentum ratios increased pressure losses and reduced the overall thermal-hydraulic benefit. Evaluation of the thermal-hydraulic PEC indicated that the combined application of Al_2O_3/CMC nanofluids and jet injection can achieve superior overall performance compared with conventional cooling approaches. The enhanced heat transfer obtained through the combined effects of shear-thinning rheology, nanoparticle addition, and jet-induced mixing resulted in improved thermal-hydraulic performance under the investigated operating conditions. The findings of this study demonstrate that jet-assisted Al_2O_3/CMC nanofluids represent a promising solution for improving heat transfer in BFS channels and other thermal systems involving separated flows. The proposed approach offers valuable potential for advanced cooling applications where high thermal efficiency and compact system design are required.

Authors' Contributions

The author solely conducted the research and prepared the manuscript and has approved its final version.

Data Availability

The data are available from the corresponding author upon reasonable request.

Funding

This work was carried out without financial support from any public, commercial, or non-profit organizations.

Conflict of Interest

There are no competing interests to declare.

Consent for Publication

The author confirms consent for the publication of this work

Ethics Approval and Consent to Participate

This article does not include experiments involving humans or animals.

References

[1] Bayareh, M. (2023). An overview of non-Newtonian nanofluid flow in macro-and micro-channels using two-phase schemes. *Engineering Analysis with Boundary Elements, 148,* 165–175. https://doi.org/10.1016/j.enganabound.2022.12.033

[2] Akbari, O. A., Toghraie, D., Karimipour, A., Marzban, A., & Ahmadi, G. R. (2017). The effect of velocity and dimension of solid nanoparticles on heat transfer in non-Newtonian nanofluid. *Physica E: Low-Dimensional Systems and Nanostructures*, *86*, 68–75. https://doi.org/10.1016/j.physe.2016.10.013

[3] Rahmati, A. R., Akbari, O. A., Marzban, A., Toghraie, D., Karimi, R., & Pourfattah, F. (2018). Simultaneous investigations the effects of non-Newtonian nanofluid flow in different volume fractions of solid nanoparticles with slip and no-slip boundary conditions. *Thermal Science and Engineering Progress*, *5*, 263–277. https://doi.org/10.1016/j.tsep.2017.12.006

[4] Shahsavani, E., Afrand, M., & Kalbasi, R. (2018). Using experimental data to estimate the heat transfer and pressure drop of non-Newtonian nanofluid flow through a circular tube: Applicable for use in heat exchangers. *Applied Thermal Engineering*, *129*, 1573–1581. https://doi.org/10.1016/j.applthermaleng.2017.10.140

[5] Bahiraei, M., & Alighardashi, M. (2016). Investigating non-Newtonian nanofluid flow in a narrow annulus based on second law of thermodynamics. *Journal of Molecular Liquids*, *219*, 117–127. https://doi.org/10.1016/j.molliq.2016.03.007

[6] Mahian, O., Kolsi, L., Amani, M., Estellé, P., Ahmadi, G., Kleinstreuer, C., ... & Pop, I. (2019). Recent advances in modeling and simulation of nanofluid flows-Part I: Fundamentals and theory. *Physics Reports*, *790*, 1–48. https://doi.org/10.1016/j.physrep.2018.11.004

[7] Maleki, H., Safaei, M. R., Alrashed, A. A. A. A., & Kasaeian, A. (2019). Flow and heat transfer in non-Newtonian nanofluids over porous surfaces. *Journal of Thermal Analysis and Calorimetry*, *135*(3), 1655–1666. https://doi.org/10.1007/s10973-018-7277-9

[8] Sabeur, A. (2026). Machine learning applications in nanofluid research: A comprehensive review of trends, challenges, and future perspectives. In *Applied intelligence*. IntechOpen. https://doi.org/10.5772/intechopen.1014076

[9] Patankar, S. (2018). *Numerical heat transfer and fluid flow*. CRC press. https://doi.org/10.1201/9781482234213

[10] Chon, C. H., Kihm, K. D., Lee, S. P., & Choi, S. U. S. (2005). Empirical correlation finding the role of temperature and particle size for nanofluid (Al_2O_3) thermal conductivity enhancement. *Applied physics Letters*, *87*(15), 153107. https://doi.org/10.1063/1.2093936

[11] Shyam, R., & Chhabra, R. P. (2013). Effect of Prandtl number on heat transfer from tandem square cylinders immersed in power-law fluids in the low Reynolds number regime. *International Journal of Heat and Mass Transfer*, *57*(2), 742–755. https://doi.org/10.1016/j.ijheatmasstransfer.2012.11.001

[12] Mosavi, A., Hekmatifar, M., Alizadeh, A. ad, Toghraie, D., Sabetvand, R., & Karimipour, A. (2020). RETRACTED: The molecular dynamics simulation of thermal manner of Ar/Cu nanofluid flow: The effects of spherical barriers size. *Journal of Molecular Liquids*, *319*, 114183. https://doi.org/10.1016/j.molliq.2020.114183

[13] Matsson, J. E. (2022). *An introduction to ANSYS fluent 2022*. Sdc Publications. https://www.sdcpublications.com/Textbooks/Introduction-ANSYS-Fluent-2022/ISBN/978-1-63057-569-4/

[14] Santra, A. K., Sen, S., & Chakraborty, N. (2009). Study of heat transfer due to laminar flow of copper--water nanofluid through two isothermally heated parallel plates. *International Journal of Thermal Sciences*, *48*(2), 391–400. https://doi.org/10.1016/j.ijthermalsci.2008.10.004

[15] Armaly, B. F., Durst, F., Pereira, J. C. F., & Schönung, B. (1983).. *Journal of Fluid Mechanics*, *127*, 473–496. https://doi.org/10.1017/S0022112083002839

[16] Sheikholeslami, M., Hatami, M., & Ganji, D. D. (2014). Nanofluid flow and heat transfer in a rotating system in the presence of a magnetic field. *Journal of Molecular Liquids*, *190*, 112–120. https://doi.org/10.1016/j.molliq.2013.11.002

[17] Menni, Y., Chamkha, A. J., & Azzi, A. (2019). Nanofluid flow in complex geometries—a review. *Journal of Nanofluids*, *8*(5), 893–916. https://doi.org/10.1166/jon.2019.1663

[18] Mahian, O., Kianifar, A., Kleinstreuer, C., Al-Nimr, M. A., Pop, I., Sahin, A. Z., & Wongwises, S. (2013). A review of entropy generation in nanofluid flow. *International Journal of Heat and Mass Transfer*, *65*, 514–532. https://doi.org/10.1016/j.ijheatmasstransfer.2013.06.010

[19] Sarfraz, M., Khan, M., Al-Zubaidi, A., & Saleem, S. (2023). Insights into the thermodynamic efficiency of Homann-Agrawal hybrid nanofluid flow. *Alexandria Engineering Journal*, *82*, 178–185. https://doi.org/10.1016/j.aej.2023.09.074

[20] Sheikholeslami, M., & Vajravelu, K. (2017). Nanofluid flow and heat transfer in a cavity with variable magnetic field. *Applied Mathematics and Computation*, *298*, 272–282. https://doi.org/10.1016/j.amc.2016.11.025

[21] Sheikholeslami, M., Bandpy, M. G., Ellahi, R., Hassan, M., & Soleimani, S. (2014). Effects of MHD on Cu--water nanofluid flow and heat transfer by means of CVFEM. *Journal of Magnetism and Magnetic Materials*, *349*, 188–200. https://doi.org/10.1016/j.jmmm.2013.08.040